International Journal of Signal and Imaging Systems Engineering

ISSN online: 1748-0701 - ISSN print: 1748-0698
https://www.inderscience.com/ijsise

Computational simulation of human fovea

Prathibha Varghese, G. Arockia Selva Saroja

DOI: 10.1504/IJSISE.2023.10059440

Article History:

Received:	28 May 2021
Accepted:	21 October 2022
Published online:	28 September 2023

Copyright © 2023 Inderscience Enterprises Ltd.

Computational simulation of human fovea

Prathibha Varghese* and G. Arockia Selva Saroja

Electronics & Communication Department,
Noorul Islam Centre for Higher Education,
Tamil Nadu, 629180, India
Email: prathibhavarghese2003@gmail.com
Email: aroseg@yahoo.com
*Corresponding author

Abstract: Many metaheuristic algorithms have been developed with genuine inspiration from nature. Photoreceptors through certain ganglion cells of fovea towards the main cells of said visual cortex, every physical optical system is modelled in the form of cascading sub-filters. This idea has sparked research into the biological retina to better understand its information-processing capacities to copy the architecture to create mechanical visual sensors. Human fovea photoreceptor cones and rods have a hexagonal rather than a rectangular shape. In that context, we provide a 2-D interpolation lattice conversion approach for creating hexagonal meshes, which is guaranteed to maintain alignment with our visual system and has a straightforward implementation and calculation process. This approach delivers a simulated hexagonal image for visual verification without needing a hexagonal capture or display device.

Keywords: hexagonal image; spiral architecture; hexagonal pixels; HVS; square pixels; square pixels; hexagonal sampling; hexagon symmetry; connectivity; equidistance; angular resolution.

Reference to this paper should be made as follows: Varghese, P. and Selva Saroja, G.A. (2023) 'Computational simulation of human fovea', *Int. J. Signal and Imaging Systems Engineering*, Vol. 12, No. 4, pp.158–166.

Biographical notes: Prathibha Varghese received her BTech degree in Electronics and, Communication Engineering from M.G University, India in 2005, and, MTech degree in VLSI and Embedded Systems from CUSAT, India in 2010. She is currently a part-time PhD student and working towards a PhD degree, in Digital Image Processing at Noorul Islam Centre for Higher, Education (NICHE), Tamil Nadu, Department of Electronics and, Communication Engineering. Her research interests include image, processing, computer vision machine learning, and deep learning.

G. Arockia Selva Saroja received her BE degree in Electronics and Communication, Engineering from Manonmaniam Sundaranar University, India in 1997 and ME degree, in Communication Systems from Madurai Kamaraj University, India, in 1998 and PhD, degree from Noorul Islam Centre for Higher Education, India, in 2017. She is currently working as an Associate Professor in the Department of Electronics and Communication, Engineering. She has been working in the institution since 1997 and has got 15 years of, research experience. Her research includes medical image processing, computer vision, machine learning and wireless networks.

1 Introduction

In the swiftly developing field of image processing and computer vision, natural computing has come to light as a potential remedy for up-and-coming researchers. By taking inspiration from the natural world, nature-inspired computing (NIC) (Yang and Cui, 2014) has created numerous innovative algorithms and calculations. Numerous in-depth studies are being advanced in the hexagonal tessellation lattice to bring about a breakthrough in digital image processing. 'nature-inspired computing' (NIC) methods are more adaptable, versatile, reliable, quick to deliver, and simple to understand. It can therefore be used to solve various mathematical computations and real-time applications.

Machine vision sensor placement should mimic the dense cone as well as rod distribution within the human Fovea, to duplicate the properties of HVS (Ahir et al., 2019). Today, rectangular meshes are preferred over hexagonal ones because they are simpler to create in hardware, more readily available, and more widely understood to work with the cartesian coordinate system. Given that, as shown in Figure 1, hexagonal pixels nearly mimic the form of the human The human visual system and hexagonal geometry have a close relationship, Fovea. The hexagonal lattice is frequently found in nature, including in beehives, dragonfly eyes, bubble rafts, and other structures (Buschbeck et al., 1999). Here's a basic explanation of how the human eye captures images. Located mostly in the backside of the eye, this retina seems to be a thin layer of tissue

Copyright © 2023 Inderscience Enterprises Ltd.

that is extremely sensitive to damage. The retina's function is to receive visual information from the eye and transform it all into neural activity which may be conveyed to the brain further for analysis. The fovea is a small area of the retina where rods as well as cones are organised inside a hexagonal grid. A hexagonal lattice has an added benefit over a square one when it comes to more accurately distinguishing between straight and curved edges because of this type of spatial organisation (Middleton and Sivaswamy, 2006; Sheridan et al., 2000).

Figure 1 Human fovea photoreceptor rods and cons

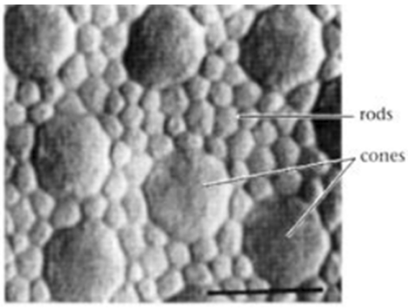

In many cases, it is pretty challenging to construct a spatial geometric distribution that mimics HVS from a 2-D image to attain real-time performance Wang et al. (2005). According to its simplicity in the coordinate system cartesian as well as its orthogonal alignment, rectilinear squares mesh is widely employed in sensing devices & display panels. The square mesh, however, falls short of requirements that call for symmetric geometric computation between contiguous close-by pixels. Here, it is necessary to look into a substitute that would be appropriate for the challenge (Asharindavida et al.,2012). Mechanical visual sensors that are readily available come close to matching the retinal photoreceptor density of primates. Regarding range and sensor-level processing power, they still fall short of the human visual system. This spark spurred current research on biological retinas to learn more about processing methods to create the best possible visual sensors Constandinou (2005). According to Jeevan and Krishnakumar (2016), three standard lattice systems are squares, triangles, and hexagons. With the help of these tessellation patterns, we can tile a plane with no overlap and empty areas in between. All other tessellation spatial arrangements will be based on the inconsistent spacing among pixels in the neighbourhood and samples will overlap.

Figure 2 Schemes of standard tessellation: (a) square, (b) triangle and (c) hexagon (see online version for colours)

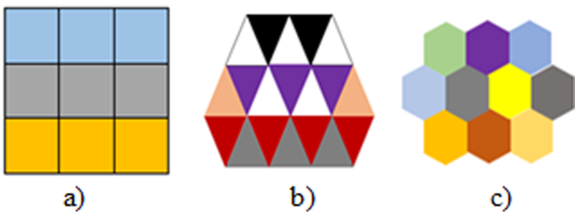

The most typical and straightforward tessellation that fits the cartesian coordinate system is thought to be Figure 2(a). This triangular tessellation in Figure 2(b) is more densely packed than square tessellations. The most successful tessellation scheme that complies with the HVS is considered hexagonal tessellation, as depicted in n Figure 2(c). The uniform neighbourhood pixels, greater packing density, equidistant neighbourhood connectedness, and enhanced angular rectification are only a few of the geometric advantages. Additionally, from the primate's perspective, human anatomy cognition is what gives this geometric arrangement its added value (Schwartz, 1980). A set of hexagonal pixels is formed by the image on the 2-D image frame, and this configuration produces acute eyesight for information gathering. The number of retinal photoreceptors in primates' retinas can be closely matched by mechanical vision sensors that are widely available. They still lack the range and sensor-level processing power of the human visual system. These benefits increase accuracy when detecting curved and straight edges (Scotney and Coleman, 2007). According to Tam (2014), traditional square architecture displays 3X3 matrix units, whereas hexagonal architecture is structured in sets of 7 hexagons (Figure 3).

Figure 3 Architecture of pixels: (a) hexagon and (b) square (see online version for colours)

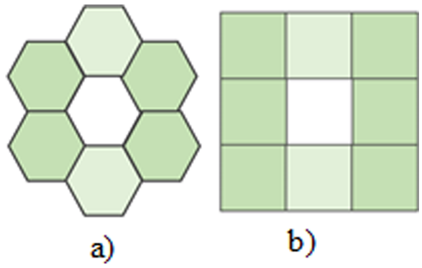

The Cartesian coordinate systems only work with traditional square lattice images. To address and store data effectively, the hexagonal grid image system needs an appropriate coordinate system. Three coordinate symmetrical coordinate frames (Her, 1995), a single indexing scheme (Sheridan et al., 2000), and a scheme of both oblique coordinate axes addressing (Luczak and Rosenfeld, 1976) are three prominent addressing strategies that connect the hexagonal structure in Figure 4.

Each hexagonal pixel is represented by an ordered pair of vectors in horizontal and vertical directions with the aid of a two-axes oblique system coordinate (see Figure 4(a)). The advantages of this system are as follows (Coleman et al., 2009a, 2009b):

- *complete*: a point can be efficiently and precisely portrayed in 2-dimensional space
- *unique*: a point representation can be given an exact ordered pair of coordinates
- *convertible*: the Cartesian coordinate system is comparable to it and may be changed into and out of it rapidly.

Her (1992), Her and Yuan (1994) propose the three-axe coordinate frame, commonly known as the symmetrical hexagonal coordinate frame.

As depicted in Figure 4(b), the mentioned coordinate system utilises x, y and z coordinates. Additionally, a one-to-one mapping symmetrical hexagonal frame (*R3) and three-dimensional cartesian frame (R3), shown in Figure 4. Any 3 coordinates will adhere to the mathematical formula shown in equation (1). The adjacent pixels are separated by a unit distance.

$$x + y + z = 0 \tag{1}$$

All geometric transformations and theoretical explanations can be easily transferred to and from *R3 to R3 because of the symmetrical hexagonal coordinate frame's proximity to and interaction with three dimensions. In this method, the structural symmetry feature is well preserved.

Figure 4 Schematic of hexagonal coordinates a) two-axes oblique b) three coordinates symmetrical *R^3 c) *R^3 and R^3 d relationship) single indexing-spiral architecture (see online version for colours)

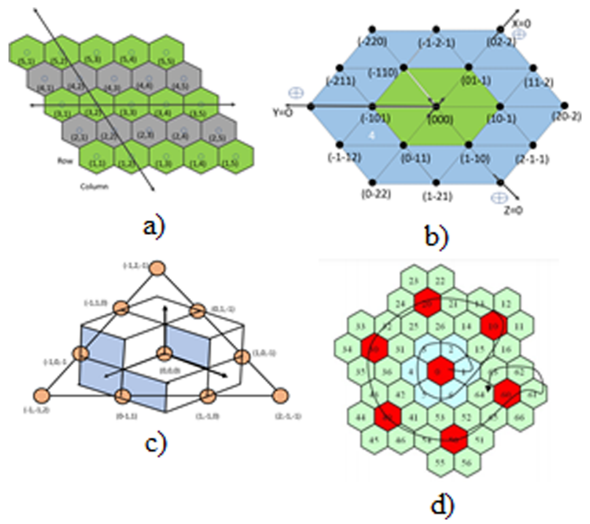

Spiral addressing (SA), created by Middleton and Sivaswamy (2006) and Wu et al. (2002), is another addressing strategy for hexagonal structures. SA is based on a single addressing system. Spiral clusters of hexagonal pixels are used. Each pixel in spiral addressing consistently has six adjacent pixels. As indicated in Figure 4(d), In SA, the first step is to assign a destination identifier to each hexagon, starting on the image centre and increasing as seventh powers.

Figure 5 Cluster of basic seven hexagonal cells (see online version for colours)

The address is initially put to a row of seven hexagons with the labels 0, 1, 2, 3, 4, and 6. The framework is widened to accommodate an extra 6 hexagons, as seen in Figure 5. Each address in this case is multiplied by 10. As it has been done for the first seven hexagons, an address is given for each newly placed hexagon concerning the centre pixel address (Narayanankutty and Raffi, 2014).

The cluster of size $7n$ comprises the numbered hexagons (n = 1, 2, 3, ...). The hexagons tile the plane along the spiral rotation in a recursive spiral-modular pattern. 49 pixels are presented in a one-dimensional addressing method as seen in Figure 4(d). Many computer vision applications benefit from this architecture's extra feature of establishing the image's centre at its origin and maintaining connectivity throughout its six neighbourhoods. In this study, we employ a two-axes oblique coordinate system because it can successfully recreate a hexagonal grid using hardware already in use.

The research work is prepared with the following organisational structure. The literature review of hexagonal image processing is summarised in Section 2. The representation, processing, and hexagonal picture lattice are all covered in Section 3. The suggested 2-D interpolation lattice conversion pseudo hexagonal simulation algorithm, known as the "PA" algorithm, is described in Section 4 (Where P represents the first author's first letter and A represents the second author's first letter). Section 5 contains the findings and discussions. Our conclusion will be presented in Section 6, along with details on any possible subsequent works in the future.

2 Literature review

Although using hexagonal images has several advantages, the limitation of its utilisation is primarily a result of outdated technology, featuring hexagonal image sensors, as well as hexagonal picture displays. Building a successful resampling method will allow us to use the benefits that hexagonal lattice offers for image processing while continuing research developments in this technology employing the currently available hardware. We must use a resampling technique to carry out tasks for display and processing with the hardware we currently have (Gardiner et al., 2016). The pixels are not grouped in a spiral pattern in a true hexagonal configuration. Instead, numerous coordinate systems and addressing algorithms are created to mimic hexagonal grids (Luczak and Rosenfeld, 1976; Her, 1995).

Here, we go over the specifics of hexagonal sampling and the numerous resampling techniques developed in the literature to make it possible to switch from one lattice to another lattice grid.

2.1 Hexagonal sampling

Mersereau (1979) state that there are several problems with rectangular space sampling, including the fact that the spatial resolution changes depending on the direction of the sample. Since this is the case, the best example pattern is a regular hexagonal arrangement. As can be shown in Figure 15, if a signal is bandlimited during a circular region of the Fourier planes, the most effective sampling method is a hexagonal one. When evaluating signals of the same kind, Huck et al. (1990)

found that hexagonal sampling required 13.4% points fewer repetitions over rectangular selection.

$$x(n_1, n_2) = x_a(n_1T_1, n_2T_2) \tag{2}$$

where x_a (T_1, T_2) is analogue images, and T_1 and T_2 denote sampling intervals in horizontal as well as vertical directions. The rectangular sampling sequence was represented by $x(n_1, n_2)$.

Let x_a (Ω_1, Ω_2) represents Fourier transformation of x_a (T_1, T_2).under condition: x_a (Ω_1, Ω_2)=0, (Ω_1, Ω_2) €R, then we can say the image is bandlimited as shown in Figure 15(a). Additionally, the image can be precisely rebuilt with equation (3).

$$T_1 < \frac{\pi}{w_1} \, and \, T_2 \frac{\pi}{w_2} \tag{3}$$

where w_1 and w_2 represent the horizontal and vertical bandwidth expressed in radians.

Similar to rectangular sampling, hexagonal sampling can be shown. It can be represented in equation (4).

$$x(n_1, n_2) = x_a\left(\frac{2n_1 - n_2}{2}T_1, n_2T_2\right) \tag{4}$$

where $x(n_1, n_2)$ displays the image that was hexagonally sampled in Figure 15(b). It needs to be band-restricted using a hexagonal band region to precisely recover the original image with equation (5).

$$T_1 \leq \frac{4\pi}{2w_1 + w_2} \, and \, T_2 \leq \frac{\pi}{w_2} \tag{5}$$

which may not have the same horizontal and vertical sampling intervals (Gardiner et al.,2007).

Figure 6 (a) Rectangular sampling, (b) hexagonal sampling (see online version for colours)

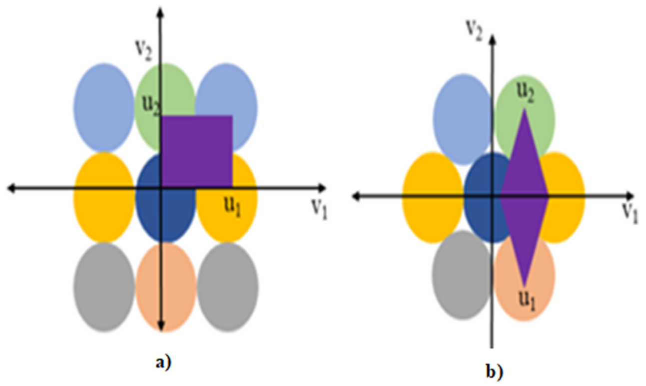

3 Resampling methodology

3.1 Alternate pixel suppressant method

According to Sankar et al. (2004), a hexagonal grid can be created over a rectangular grid by alternately eliminating the rectangular grid's horizontal rows and vertical columns. The equation for the subsampling is given in equation (2). The equation for subsampling is given in equation (6).

$$pixel\_val_{hex(i,j)} = \begin{cases} pixel_{val(2*i,2*j)}, & if\ is\ even \\ pixel_{val(2*i,2*j+1)} & if\ i\ is\ odd \end{cases} \tag{6}$$

Since part of the pixels in the rectangular grid and the hexagonal grid are suppressed, this method has no one-to-one correspondence. The pixels that are silenced are given zero values. The suppressed pixels are not considered while performing computations with the sub-sampled pictures. As shown in Figure 7, compared to a rectangular grid, newly sampled parts include a pixel quarter.

Figure 7 Pixel arrangement (a) rectangular and (b) sub-sampled hexagonal mesh (see online version for colours)

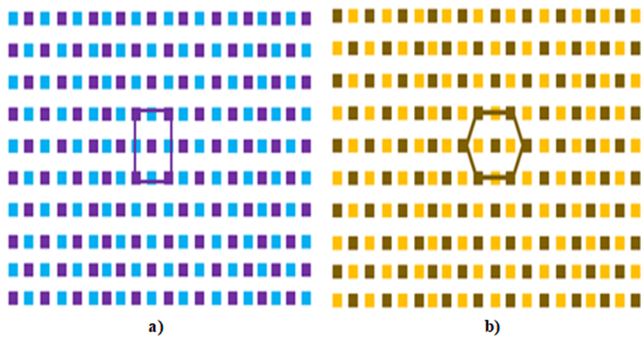

3.2 Half-pixel shift method

For hexagonal mapping from a square, Periaswamy (1996) suggested a half-pixel shift method in which the midpoint of each odd line is calculated with a simple step (i.e., midpoint = 1/2(left pixel + right pixel)), with these extreme right, as well as left measurements, discarded and the midpoint values retained as shown in Figure 8. The hexagonal mapping equation is given in equations (7) and (8) (Gardiner et al., 2011).

$$p^{new}(x, 2y) = p^{old}(x, 2y) \tag{7}$$

$$p^{new}(x, 2y+1) = \frac{p^{old}(x, 2y+1) + p^{old}(x+1, 2y+1)}{2} \tag{8}$$

4 Features of hexagonal sampling scheme

4.1 More efficient sampling scheme

An inadequate sampling rate is referred to as aliasing, and it causes undesired consequences in the recovered signal (Burton et al., 1993). On such a hexagonal grid, regenerating an input signal with a low wave number takes fewer samples, according to a study by Petersen and Middleton (1962). The main conclusion is that the square lattice sampling strategy is ineffective. As a result, the rhombic hexagon (120°) is regarded as an efficient sampling lattice when utilising a two-dimensional isotropic function, as shown in Figure 9. In this figure, the spectrum is circumscribed by circles with a radius of 2B. The distance between the sample sites is determined by 1/(3*B). The resulting sample efficiency is 90.8% as opposed to the typical square lattice's 78.5%.

Figure 8 Hexagonal mapping using half-pixel shift method: (a) square mapping and (b) hexagonal mapping (see online version for colours)

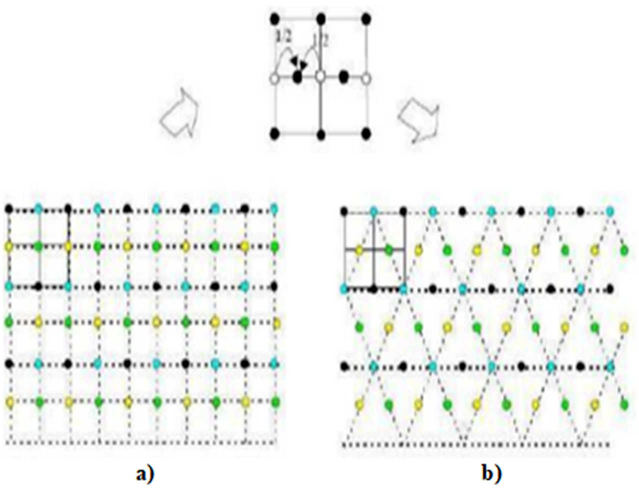

Figure 9 Sampling lattice of (a) circular and (b) isotropic function (see online version for colours)

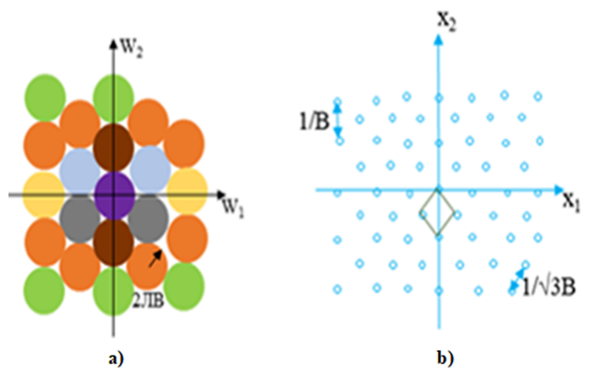

4.2 Smaller quantisation error

In the most modern digital technology, the quantisation of an image into spatial units with finite dimensions known as pixels is crucial. The quantisation error is a crucial factor in determining the value of the layout of the many accessible sensors. Petersen and Middleton (1962), Kamgar-Parsi and Kamgar-Parsi (1993), Kamgar-Parsi and Sander (1989), Kamgar-Parsi (1992) created an equation to calculate hexagonal lattice quantisation error and which is lesser than with a square.

4.3 Consistent connectivity

The interconnectivity between the pixels is the core idea in digital image processing. According to Richard and

Figure 10 Spectral packaging for (a) square (b) hexagonal (see online version for colours)

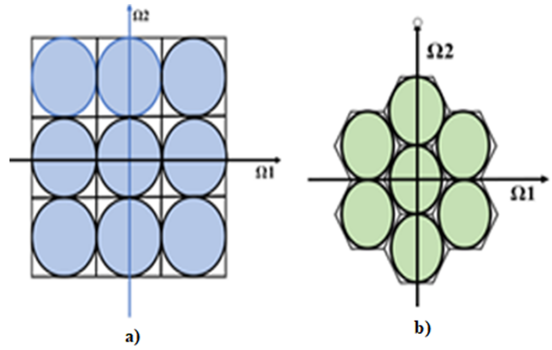

Gonzalez (2001), two pixels are connected if they are neighbours and meet the required similarity standard. There is a two-pixel neighbourhood in a square grid. If two pixels have the same corner or share an edge, we consider them to be linked. As shown in Figure 11(a) and (b), a square grid has four neighbourhood pixels and eight neighbourhood pixels, respectively. However, there is no option for connectedness in the case of a hexagonal grid (Mylopoulos and Pavlidis, 1971; Golay, 1969). We can only define a 6-neighbourhood connection, as shown in Figure 11c. Numerous image processing algorithms can be implemented quickly and effectively because there is a lack of communication options. The hexagonal grid's neighbourhood connectedness is constant and limited to six directions.

Figure 11 Neighbouring pixels in (a) square and (b) hexagonal lattices (see online version for colours)

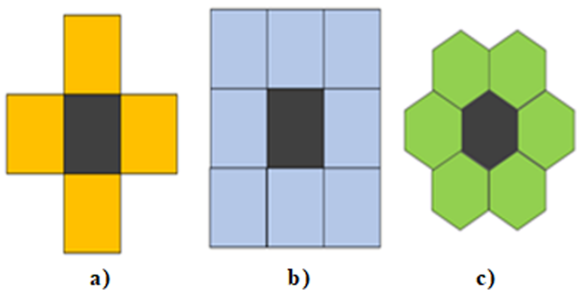

4.3.1 Equidistance

The standard square lattice image considers two separate categories of distance measurements. As shown in Figure 12(a), the computed distance between neighbouring pixels in diagonal orientations is approximately two times that of the corresponding horizontal direction. As illustrated in Figure 12(b), each hexagon in a hexagonal grid has a consistent number of six neighbours, all of whom are evenly spaced from the centre pixel along its six edges (He et al., 2007).

4.3.2 Greater angular resolution

Because hexagonal lattice has better angular resolution than square lattice, it has become more advantageous.

According to Serra (1986), consecutive pixels in a hexagonal lattice are separated by 60 rather than 90 pixels. Curved features can be expressed more effectively in hexagonal shapes than square ones, as seen in Figure 13(a). In hexagonal lattices, the consistent connection has resulted in improved angular resolution.

Figure 12 Distance measure for (a) square (b) hexagon (see online version for colours)

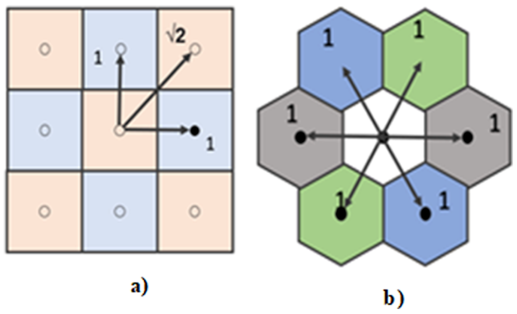

Figure 13 Curved feature representation in (a) hexagonal and (b) square (see online version for colours)

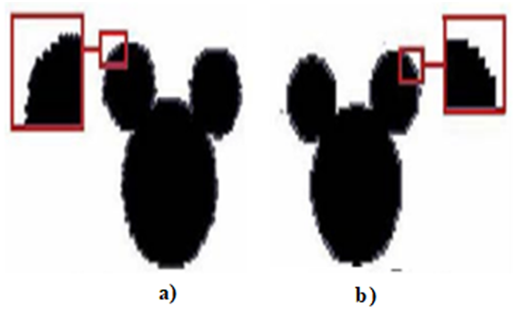

Figure 14 Symmetries in structure (a) square symmetry and (b) hexagon symmetry (see online version for colours)

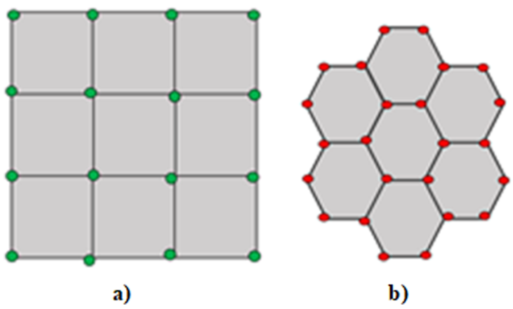

4.4 Higher symmetry

The symmetry of a hexagonal grid is the same at all angles (0, 60, and 120). Numerous image processing applications get more value due to this added benefit. For instance, a hexagonal grid will retain more image information than a square grid when we rotate the photographs on it. Jeevan and Krishnakumar (2016) created a variety of morphological operators. Due to the continuous connection and more excellent symmetry of the hexagonal grid, as depicted in Figure 14, he favours it above the square grid.

5 Flow diagram of psuedo hexagonal processing

To further study the subject of hexagonal image processing, square latticed images must now be resampled or converted to hexagonal latticed images. According to Middleton and Sivaswamy (2001), each pixel is represented by a block of nxn pixels in this novel method. The processing of images in a virtual hexagonal environment uses subpixel hexagonal images. This technique for transforming square grid images into hexagonal grid images, as illustrated in Figure 17, uses hexagonal image processing, which is employed immediately for modern life since hexagonal image sensors are not readily available.

Figure 15 Processing of hexagonal images (see online version for colours)

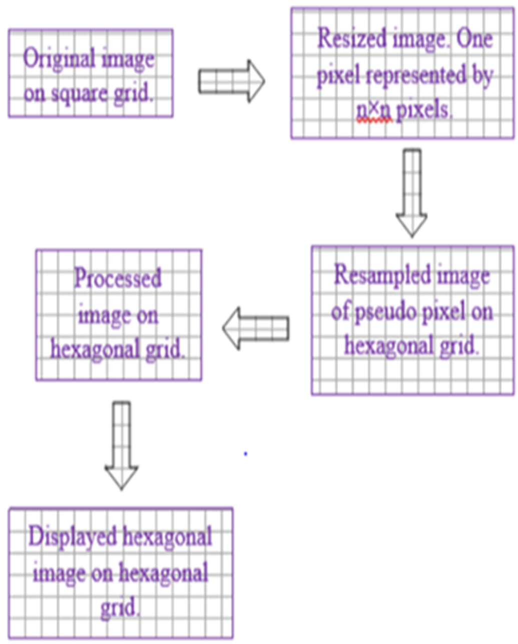

Resampling results in a sub-pixel clustering effect, which reduces the impact of resolution loss. Each hexagonal pixel is represented as a block of 66 pixels.

The selection of the hexagonal pixel's associative, which is independently gathered, is influenced by two policy considerations:

- There should be no gaps between pixels that are neighbours in six dimensions.
- The arrangement of the pixels must resemble a hexagon. A hexagonal pixel lattice, for example, should follow the geometry's rules (Gardiner et al., 2011).

5.1 Simulation of hexagonal pixel

Currently, pseudo software implementation is used to resample rectilinear square pixel-centered images to simulate hexagonal images. With this suggested approach, hexagonal square-shaped 'sub-pixels' are combined to form a 'pixel', which is the final product. Every pixel is embodied using an nXn block of pixels throughout to facilitate sub-pixel clustering as well as realise the correct resolution. As seen in Figure 16, the hexagonal picture is constructed by mapping every pixel of said input image onto a 6x6 pixel block. This section matches the brightness of the picture's square grid exactly. If the scaling was successful, the output picture will have the same pixel density as the source. Square pixels are used to produce six pixels with the number 1, and the remaining pixels with the number 0 are eliminated.

Figure 16 Square pixels are arranged into hexagons (see online version for colours)

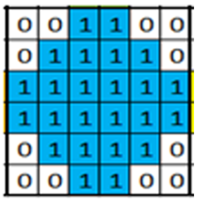

Using this technique, it is possible to transform any input picture with square pixels into one with hexagonal ones. We then set up each cluster of hexagonal pixels on the grid in the manner depicted in Figure 19. First row, first column A is displayed in pixel-shaded yellow (1,1) and pixel-shaded green (1,2). Similar to how the pixels above are numbered, the hexagonally constructed image is displayed in Figure 17.

Figure 17 Collection of hexagonal pixels (see online version for colours)

5.2 *Proposed algorithm*

The 2-D interpolation proposed algorithm for getting a cluster of hexagonal pixels steps are detailed below.

1. 1. To start.
2. Accept the selected dataset and type that is supported (*jpg, *png, *bmp).
3. Resize pictures into a single standard dataset size.
4. A null matrix is created with a 6 x6 size.
5. Find pixels coordinates indicated by the number 1, then fill them with the corresponding image pixel intensities.
6. Increase the size of the zero matrices to six times larger than the original images.
7. Put representing pixel image intensity values in the respective places.
8. Step 8: Calculate the values of the pixels that need to be shifted without overlapping, then perform the shifting operations as necessary.
9. Step 9: Adjust the pixels until they precisely line up with the neighbouring pixels.
10. Step 10: Obtain the image with the hexagonal structure.
11. Step 11: End.

Using the method outlined above, the square dataset can be changed to the hexagonal dataset. It uses a row-column addressing scheme based on an oblique two-axis reference frame, allowing us to process the picture with current hardware. The row-column addressing used in our suggested technique is modelled after the well-known Cartesian coordinate system. Using the 'PA' method, you may simulate hexagonal pixels on a colour image. Given that a colour image has three channels, an algorithm should be executed to each RGB channel separately, and the results superimposed.

6 Results and discussions

The system specification and simulation outcomes for the proposed project were demonstrated using Python and are given below:

Tool used : Python 3.8

OS : Windows 7

Processor : Intel

RAM : 8GB RAM

Dataset : CINIC-10, COIL-100, D-COIL-100 (Luo et al., 2019)

The 'PA' Algorithm produced several outstanding benefits for hexagonal picture representation, including:

- no interpolation filters are required for image enhancement
- all the adjacent pixels are similar
- unused pixels in the algorithm are less than 5
- image resolution is retained
- the hexagonal structure pixel formed is symmetric
- equal distances between the neighbourhood pixels and reliable communication to the centre pixel.

Figures 18–20 display the CINIC-10 image having hexagonal pixels imitation by employing the 'PA' algorithm. The hexagonal pixels can be visualised in the enlarged view.

Here images used are (cameraman.jpg,flower.jpg) of different sizes 32×32, 64×64, 128×128, 225×225, 512×512. As may be seen in Figure 21, a plot of the time it takes to complete the computation of the proposed method is very faster even for high-resolution images.

Figure 18 Simulation results of the CINIC-10 dataset using the PA algorithms (see online version for colours)

Figure 19 Simulation results of COIL-100 dataset using the PA algorithms (see online version for colours)

Figure 20 Simulation results of the D-COIL-100 dataset using the PA algorithms (see online version for colours)

Figure 21 Computational run time of images of various sizes: (a) grey-scale and (b) colour images (see online version for colours)

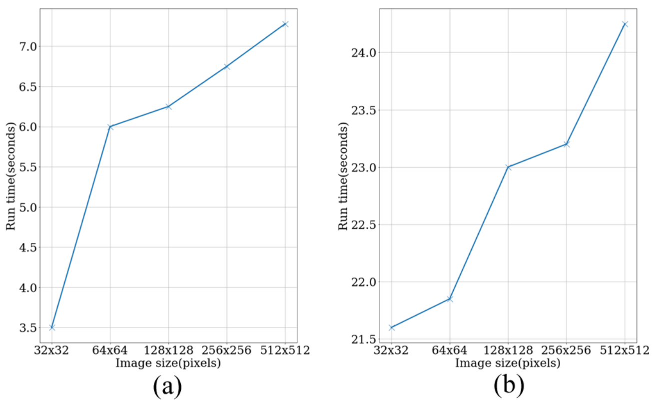

To compute the memory complexity, images (cameraman.jpg,flower.jpg) of various sizes are chosen. The memory complexity graph as shown in Figure 22 demonstrates that pseudo hexagonal images maintain clarity both in greyscale and colour images. From the perspective of space complexity, the proposed algorithm will take more space by increasing the image size.

Figure 22 Memory complexity constraint in square and hexagonal lattice comparison: (a) greyscale image and (b) colour image (see online version for colours)

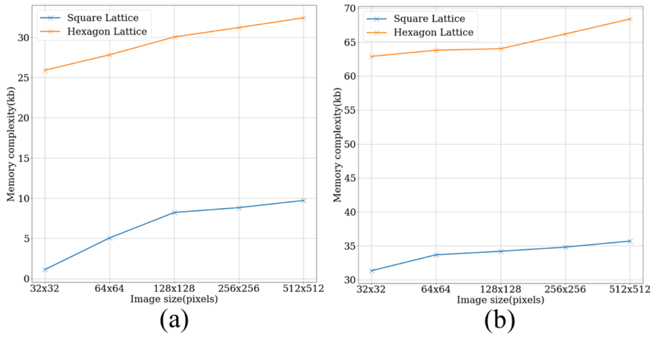

7 Conclusion

This study presents the implementation of a novel and efficient 2-D lattice interpolation hexagonal pixel simulation technique. The hexagonal pixels are produced using all the geometric advantages the structure has. Simulated hexagonal pixel geometry allows for geometrical symmetry between adjacent cells of higher order and contiguous neighbours. Although the 'PA' algorithm does not employ any interpolation filters to improve images, image resolution is kept, and the proportion of unused pixels is tiny. Additionally, this technique displays a greater representation of symmetric hexagonal pixels. The newly proposed algorithm's model of hexagonal images fits the human visual system well (HVS). The PA method's performance evaluation graph makes it abundantly evident that the suggested technique will function correctly even for high-quality photos. Although the simulation findings are promising, there is still room for improvement. This novel tessellation technique will undoubtedly open up new avenues for investigating the useful aspects of images that may aid in developing engineering, medical science, and other fields of technology that will benefit humanity. The researchers in this field are inspired by this work to use the proposed algorithm in real-world applications and calculations.

References

Ahir, T. and Satyanarayana, R.V.S. (2019) 'Three-dimensional image compression using 2.5 D spatial subsampling and reconstruction using 2.5 D morphological filters', *IUP Journal of Telecommunications*, Vol. 11, No. 1.

Asharindavida, F., Hundewale, N. and Aljahdali, S. (2012) 'Study on hexagonal grid in image processing', *Proc. ICIKM*, Vol. 45, pp.282–288.

Burton II, J.C. (1993) *End-to-End Analysis of Hexagonal vs Rectangular Sampling in Digital Imaging Systems*, The College of William and Mary.

Buschbeck, E., Ehmer, B. and Hoy, R. (1999) 'Chunk versus point sampling: visual imaging in a small insect', *Science*, Vol. 286, No. 5442, pp.1178–1180.

Coleman, S., Scotney, B. and Gardiner, B. (2009a) 'Processing hexagonal images in a virtual environment', *International Conference on Image Analysis and Processing*, Springer, Berlin, Heidelberg, pp.178–181.

Coleman, S.A., Scotney, B.W. and Gardiner, B. (2009b) *Design of Feature Extraction Operators for Use on Biologically Motivated Hexagonal Image Structures*, MVA, pp.178–181.

Constandinou, T. (2005) *Bio-Inspired Electronics for Micropower Vision Processing*, Doctoral dissertation, University of London.

Gardiner, B., Coleman, S. and Scotney, B. (2007) 'A design procedure for gradient operators on hexagonal images', *International Machine Vision and Image Processing Conference (IMVIP 2007)*, IEEE, pp.47–54.

Gardiner, B., Coleman, S. and Scotney, B.W. (2011) 'Comparing hexagonal image resampling techniques with respect to feature extraction', *14th International Machine Vision and Image Processing Conference*, Newcastle upon Tyne, Cambridge Scholars Publishing, pp.102–115.

Gardiner, B., Coleman, S.A. and Scotney, B.W. (2016) 'Multiscale edge detection using a finite element framework for hexagonal Pixel-based images', *IEEE Transactions on Image Processing*, Vol. 25, No. 4, pp.1849–1861.

Golay, M.J.E. (1969) 'Hexagonal parallel pattern transformations', *IEEE Transactions on Computers*, Vol. 100, No. 8, pp.733–740.

He, X., Li, J. and Hintz, T. (2007) 'Comparison of image conversions between square structure and hexagonal structure', *International Conference on Advanced Concepts for Intelligent Vision Systems*, Springer, Berlin, Heidelberg, pp.262–273.

Her, I. (1992) 'A symmetrical coordinate frame on the hexagonal grid for computer graphics and vision', *International Design Engineering Technical Conferences and Computers and Information in Engineering Conference*, American Society of Mechanical Engineers, Vol. 97720, pp.187–190.

Her, I. and Yuan, C-T. (1994) 'Resampling on a pseudohexagonal grid', *CVGIP: Graphical Models and Image Processing*, Vol. 56, No. 4, pp.336–347.

Her, I. (1995) 'Geometric transformations on the hexagonal grid', *IEEE Transactions on Image Processing*, Vol. 4, No. 9, pp.1213–1222.

Huck, F.O., John, S. and Reichenbach, S.E. (1990) 'Information theoretical assessment of image gathering and coding for digital restoration', *Visual Communications and Image Processing'90: Fifth in a Series*, International Society for Optics and Photonics, Vol. 1360, pp.1590–1607.

Jeevan, K.M. and Krishnakumar, S. (2016) 'An algorithm for the simulation of pseudo hexagonal image structure using MATLAB', *International Journal of Image, Graphics and Signal Processing*, Vol. 8, No. 6, p.57.

Kamgar-Parsi, B. and Kamgar-Parsi, B. (1993) 'Evaluation of quantization error in computer vision', *Physics-Based Vision: Principles and Practice: Radiometry*, Vol. 11, p.293.

Kamgar-Parsi, B. and Sander, W.A. (1989) 'Quantization error in spatial sampling: comparison between square and hexagonal pixels', *Proceedings CVPR'89: IEEE Computer Society Conference on Computer Vision and Pattern Recognition*, IEEE, IEEE Computer Society, pp.604–605.

Kamgar-Parsi, B. (1992) 'Quantization error in hexagonal sensory configurations', *IEEE Computer Architecture Letters*, Vol. 14, No. 06, pp.665–671.

Luczak, E. and Rosenfeld, A. (1976) 'Distance on a hexagonal grid', *IEEE Computer Architecture Letters*, Vol. 25, No. 05, pp.532–533.

Luo, J., Zhang, W., Su, J. and Xiang, F. (2019) 'Hexagonal convolutional neural networks for hexagonal grids', *IEEE Access*, Vol. 7, pp.142738–142749.

Mersereau, R.M. (1979) 'The processing of hexagonally sampled two-dimensional signals', *Proceedings of the IEEE*, Vol. 67, No. 6, pp.930–949.

Middleton, L. and Sivaswamy, J. (2001) 'Edge detection in a hexagonal-image processing framework', *Image and Vision Computing*, Vol. 19, No. 14, pp.1071–1081.

Middleton, L. and Sivaswamy, J. (2006) *Hexagonal Image Processing: A Practical Approach*, Springer Science & Business Media, 30 March.

Mylopoulos, J.P. and Pavlidis, T. (1971) 'On the topological properties of quantized spaces, I. the notion of dimension', *Journal of the ACM (JACM)*, Vol. 18, No. 2, pp.239–246.

Narayanankutty, K.A. and Raffi, M. (2014) 'Hardware implementation of edge detection on hexagonal sampled image grids', *International Journal of Computer Applications*, Vol. 975, p.8887.

Periaswamy, S. (1996) *Detection of Microcalcifications in Mamograms using Hexagonal Wavelets*, MS thesis, University of South Carolina.

Petersen, D.P. and Middleton, D. (1962) 'Sampling and reconstruction of wave-number-limited functions in N-dimensional Euclidean spaces', *Information and Control*, Vol. 5, No. 4, pp.279–323.

Sankar, K.P., Sanjay, T. and Rajan, E.G. (2004) 'Hexagonal pixel grid modelling and processing of digital images using clap algorithms', *International Conference on Systemic*.

Serra, J. (1986) 'Introduction to mathematical morphology', *Computer Vision, Graphics, and Image Processing*, Vol. 35, No. 3, pp.283–305.

Sheridan, P., Hintz, T. and Alexander, D. (2000) 'Pseudo-invariant image transformations on a hexagonal lattice', *Image and Vision Computing*, Vol. 18, No. 11, pp.907–917.

Schwartz, E.L. (1980) 'Computational anatomy and functional architecture of striate cortex: a spatial mapping approach to perceptual coding', *Vision Research*, Vol. 20, No. 8, pp.645–669.

Scotney, B.W. and Coleman, S.A. (2007) 'Improving angular error via systematically designed near-circular Gaussian-based feature extraction operators', *Pattern Recognition*, Vol. 40, No. 5, pp.1451–1465.

Tam, N.D. (2014) 'Hexagonal pixel-array for efficient spatial computation for motion-detection pre-processing of visual scenes', *Advances in Image and Video Processing*, Vol. 2, No. 2, pp.26–36.

Wang, H. *et al.* (2005) *VSA-based Fractal Image Compression*.

Woods, R.E. and Gonzalez, R.C. (2001) *Digital Image Processing*, 2nd ed., Addison-Wesley, November.

Wu, Q., Xianghjian, H. and Hintz, T. (2002) *Image Rotation without Scaling on Spiral Architecture*.

Yang, X-S. and Cui, Z. (2014) 'Bio-inspired computation: success and challenges of IJBIC', *International Journal of Bio-Inspired Computation*, Vol. 6, No. 1, pp.1–6.